Composite Structures 143 (2016) 130–142

Contents lists available at ScienceDirect

Composite Structures

journal homepage: www.elsevier.com/locate/compstruct

Uncertain natural frequency analysis of composite plates including effect of noise – A polynomial neural network approach

S. Dey [a,*], S. Naskar [b], T. Mukhopadhyay [c,*], U. Gohs [a], A. Spickenheuer [a], L. Bittrich [a], S. Sriramula [b], S. Adhikari [c], G. Heinrich [a,d]

[a] Leibniz-Institut für Polymerforschung Dresden e.V. (IPF), Germany
[b] School of Engineering, University of Aberdeen, United Kingdom
[c] College of Engineering, Swansea University, United Kingdom
[d] Technische Universität Dresden, Germany

ARTICLE INFO

Article history:
Available online 13 February 2016

Keywords:
Uncertainty quantification
Polynomial neural network
Stochastic natural frequency
Latin hypercube
Composite plate

ABSTRACT

This paper presents the quantification of uncertain natural frequency for laminated composite plates by using a novel surrogate model. A group method of data handling in conjunction to polynomial neural network (PNN) is employed as surrogate for numerical model and is trained by using Latin hypercube sampling. Subsequently the effect of noise on a PNN based uncertainty quantification algorithm is explored in this study. The convergence of the proposed algorithm for stochastic natural frequency analysis of composite plates is verified and validated with original finite element method (FEM). Both individual and combined variation of stochastic input parameters are considered to address the influence on the output of interest. The sample size and computational cost are reduced by employing the present approach compared to direct Monte Carlo simulation (MCS).

1. Introduction

Laminated composite plates are extensively used in aerospace, civil, marine and many other engineering applications due to the benefit of light-weightiness without compromising its strength and stiffness requirement. As modern weight-sensitive structures made of composite materials require more critical and complex design, the need for an accurate approach to assess the underlying uncertainties in the model, geometry, material properties, manufacturing process and operational environments has increased significantly. In the conventional deterministic analysis of structures, the variations in the system parameters are neglected and mean values of system parameters are used in the analysis with some factor of safety that may often lead to a conservative design. Due to the dependency on a large number of parameters in complex production and fabrication processes of laminated composite plate, the system properties can be random in nature resulting in uncertainty in the response of the laminated composite plate. Therefore, to well define the original problems and enable a better understanding and characterization of the actual behavior of the laminated composite structures, it is of prime importance that the inherent randomness in system parameters is incorporated in the analysis. To establish the reliability of such structures, application of computational power has favored the development of high-fidelity finite element models to deal with industrial problems. In spite of advances in capacity and speed of computer, the enormous computational cost of running complex, high fidelity scientific and engineering simulations makes it impractical to rely exclusively on simulation codes for the purpose of uncertainty quantification. Hence these high-fidelity models however own the drawback that they can be very time consuming so that only a few runs of the model can be affordable. Thus these models are practically unusable in computationally intensive methods such as traditional Monte Carlo simulation based approach, which needs thousands of finite element simulations. To overcome this lacuna generally surrogate based approach is utilized for uncertainty quantification of computationally intensive models.

Considerable researches based on deterministic analysis have been carried out on free vibration analysis of composite plates using classical laminated plate theory (CLPT) [1], first order shear deformation theory (FSDT) [2], higher order shear deformation theory (HSDT) [3] and three-dimensional (3-D) elasticity theory [4]. A considerable volume of literature is available on different analyses of laminated composites considering both deterministic [5–8] and

* Corresponding authors.
E-mail addresses: infosudip@gmail.com (S. Dey), mukhopadhyay.mail@gmail.com (T. Mukhopadhyay).
URLs: https://sites.google.com/site/drsudipdey/ (S. Dey), http://www.tmukhopadhyay.com (T. Mukhopadhyay).

http://dx.doi.org/10.1016/j.compstruct.2016.02.007
0263-8223/

stochastic [9–12] approaches. Based on higher-order theory, Naveenthraj et al. [13] studied the linear static response of graphite–epoxy composite laminates with randomness in material properties by using combination of finite element analysis and Monte Carlo simulation (MCS). Further Salim et al. [14] examined the effect of randomness in material properties such as elastic modulus Poisson's ratios etc. on the response statistics of a composite plate subjected to static loading using CLPT in conjunction with first order perturbation techniques (FOPT). Onkar and Yadav [15] investigated the nonlinear response statistics of composite-laminated flat panels with random material properties subjected to transverse random loading based on CLPT in conjunction with FOPT. Giunta et al. [16] studied the free vibration of composite plates using refined theories accounting for uncertainties. The random vibration problem deals with big data of several stochastic input parameters wherein the dimension of stiffness matrix and number of iteration reduces the computational efficacy. The curse of dimensionality is a potential challenge related with the fact that the convergence of any estimator to the true value of a smooth function defined on a space of high dimension is very slow. This means that, a priori, an ample amount of observations are required to obtain a good estimated function of the parameter of interest. This problem can be solved by using suitable reduced order model (ROM). Many researchers used ROM in different applications such as high dimensional model representation (HDMR) [17,18], Kriging [19,20], artificial neural network [21,22], polynomial regression model [23–25]. Fuzzy uncertainty propagation in composites using Gram–Schmidt polynomial chaos expansion is reported recently [26]. Relatively little efforts have been made in the past by the researchers and investigators on using polynomial neural network (PNN) model for the prediction of random system properties. Zjavka [27] employed the polynomial neural network model for forecasting the correct wind speed while Gómez-Ramírez et al. [28] investigated on forecasting time series with a new architecture for polynomial artificial neural network. Zhang et al. [29] studied the cross-validation based weights and structural analysis by Chebyshev-polynomial neural networks. Xin et al. [30,31] investigated on monotonicity and convergence of asynchronous update gradient method and with penalty using ridge polynomial neural network while Roh et al. [32,33] studied on fuzzy linear regression and radial basis function based on PNN. Recently, Huang et al. [34], Oh et al. [35] and Fazel Zarandi et al. [36] also studied the fuzzy polynomial neural networks with respective applications. Maric [37] introduced the self-organizing polynomial neural networks for solving the optimization problem while Dorn et al. [38] studied on group method of data handling (GMDH) – polynomial neural network-based method to predict approximate three-dimensional structures of polypeptides. To the best of the authors' knowledge, there is no literature covering the uncertainty quantification of natural frequencies in laminated composite structures using the polynomial neural network model. Moreover, the analysis of noise on such surrogate based uncertainty quantification algorithms is first attempted in this study.

In the present study, stochastic natural frequencies of laminated composite plates are analyzed in the presence of small random variation in the systems input variables. A polynomial neural network model is developed to reduce the computational time with adequate level of accuracy. The finite element formulation in conjunction with PNN model is thereby utilized to map the variation of responses of interest for randomness in layer-wise input parameters with different level of noise.

2. Mathematical formulation

Consider a rectangular composite laminated cantilever plate of uniform length L, width b, and thickness t, which consists of three plies located in a three-dimensional Cartesian coordinate system (x, y, z), where the x–y plane passes through the middle of the plate thickness with its origin placed at the corner of the cantilever plate as shown in Fig. 1. The composite plate is considered with uniform thickness with the principal material axes of each layer being arbitrarily oriented with respect to mid-plane. If the mid-plane forms the x–y plane of the reference plane, then the displacements can be computed as

$$\begin{aligned} u(x,y,z) &= u^0(x,y) - z\theta_x(x,y) \\ v(x,y,z) &= v^0(x,y) - z\theta_y(x,y) \\ w(x,y,z) &= w^0(x,y) = w(x,y), \end{aligned} \tag{1}$$

Assuming u, v and w are the displacement components in x-, y- and z-directions, respectively and u^0, v^0 and w^0 are the mid-plane displacements, and $\theta_{\boldsymbol{x}}$ and $\theta_{\boldsymbol{y}}$ are rotations of cross-sections along the x- and y-axes. The strain-displacement relationships for small deformations can be expressed as

$$\varepsilon_x = \frac{\partial u^o}{\partial x} - z\frac{\partial^2 w^o}{\partial x^2}, \quad \varepsilon_y = \frac{\partial v^o}{\partial y} - z\frac{\partial^2 w^o}{\partial y^2} \\ \text{and} \quad \gamma_{xy} = \frac{\partial u^o}{\partial y} + \frac{\partial v^o}{\partial x} - z\frac{2\partial^2 w^o}{\partial x \partial y} \tag{2}$$

which in matrix form can be expressed as

$$\begin{Bmatrix} \varepsilon_x \\ \varepsilon_y \\ \gamma_{xy} \end{Bmatrix} = \begin{Bmatrix} \varepsilon_x^o \\ \varepsilon_y^o \\ \gamma_{xy}^o \end{Bmatrix} + z\begin{Bmatrix} k_x \\ k_y \\ k_{xy} \end{Bmatrix} \tag{3}$$

where $\varepsilon_x^0, \varepsilon_y^0, \gamma_{xy}^0$ are the strains in the reference plane and k_x, k_y, k_{xy} are the curvatures of reference plane of the plate. The random in-plane forces and moments acting on small element and the transverse shear forces (per unit length) are

$$N_x(\overline{\omega}) = \int_{-t_b(\overline{\omega})}^{t_t(\overline{\omega})} \sigma_x dz, \; N_y(\overline{\omega}) = \int_{-t_b(\overline{\omega})}^{t_t(\overline{\omega})} \sigma_y dz, \; N_{xy}(\overline{\omega}) = \int_{-t_b(\overline{\omega})}^{t_t(\overline{\omega})} \tau_{xy} dz$$
$$M_x(\overline{\omega}) = \int_{-t_b(\overline{\omega})}^{t_t(\overline{\omega})} z\sigma_x dz, \; M_y(\overline{\omega}) = \int_{-t_b(\overline{\omega})}^{t_t(\overline{\omega})} z\sigma_y dz, \; M_{xy}(\overline{\omega}) = \int_{-t_b(\overline{\omega})}^{t_t(\overline{\omega})} z\tau_{xy} dz$$
$$V_x(\overline{\omega}) = \int_{-t_b}^{t_t} \tau_{xz} dz \text{ and } V_y(\overline{\omega}) = \int_{-t_b}^{t_t} \tau_{yz} dz \tag{4}$$

The stress–strain relationship for each ply can be expressed in matrix form

$$\begin{Bmatrix} \sigma_x \\ \sigma_y \\ \tau_{xy} \end{Bmatrix} = [\overline{Q}_{ij}(\overline{\omega})] \begin{Bmatrix} \varepsilon_x \\ \varepsilon_y \\ \gamma_{xy} \end{Bmatrix} \tag{5}$$

where $[\overline{Q}_{ij}(\overline{\omega})]$ is the stiffness matrix of the ply in x–y co-ordinate system and expressed as

$$[\overline{Q}_{ij}(\overline{\omega})] = \begin{bmatrix} m^4 & n^4 & 2m^2n^2 & 4m^2n^2 \\ n^4 & m^4 & 2m^2n^2 & 4m^2n^2 \\ m^2n^2 & m^2n^2 & (m^4+n^4) & -4m^2n^2 \\ m^2n^2 & m^2n^2 & -2m^2n^2 & (m^2-n^2) \\ m^3n & mn^3 & (mn^3-m^3n) & 2(mn^3-m^3n) \\ mn^3 & m^3n & (m^3n-mn^3) & 2(m^3n-mn^3) \end{bmatrix} [Q_{ij}] \tag{6}$$

Here $m = \sin\theta(\overline{\omega})$ and $n = \cos\theta(\overline{\omega})$, wherein $\theta(\overline{\omega})$ is the random fibre orientation angle. However, laminate consists of a number of laminae wherein $[Q_{\boldsymbol{ij}}]$ and $[\overline{Q}_{ij}(\overline{\omega})]$ denotes the on-axis elastic constant matrix and the off-axis elastic constant matrix, respectively. In matrix form, the in-plane stress resultant $\{N\}$, the moment resultant $\{M\}$, and the transverse shear resultants $\{Q\}$ can be expressed as

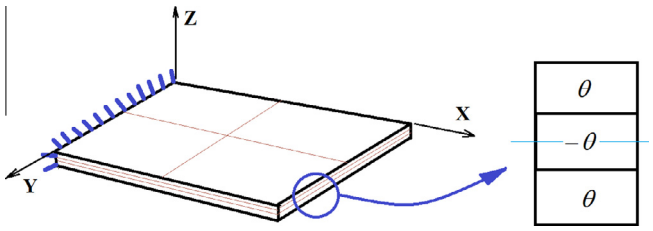

Fig. 1. Laminated composite cantilever plate.

$$\{N\} = [A]\{\varepsilon^0\} + [B]\{k\} \quad \text{and} \quad \{M\} = [B]\{\varepsilon^0\} + [D]\{k\}$$
$$\{Q\} = [A^*]\{\gamma\}$$
$$[A_{ij}^*] = \int_{-t_b(\overline{\omega})}^{t_t(\overline{\omega})} \overline{Q}_{ij} dz \quad \text{where } i,j = 4,5 \tag{7}$$

The elasticity matrix of the laminated composite plate is given by,

$$[D'(\overline{\omega})] = \begin{bmatrix} A_{ij}(\overline{\omega}) & B_{ij}(\overline{\omega}) & 0 \\ B_{ij}(\overline{\omega}) & D_{ij}(\overline{\omega}) & 0 \\ 0 & 0 & S_{ij}(\overline{\omega}) \end{bmatrix} \tag{8}$$

where

$$[A_{ij}(\overline{\omega}), B_{ij}(\overline{\omega}), D_{ij}(\overline{\omega})] = \sum_{k=1}^{n} \int_{z_{k-1}}^{z_k} [\overline{Q}_{ij}(\overline{\omega})]_k [1, z, z^2] dz, \quad i,j = 1,2,6 \tag{9}$$

$$[S_{ij}(\overline{\omega})] = \sum_{k=1}^{n} \int_{z_{k-1}}^{z_k} \alpha_s [\overline{Q}_{ij}(\overline{\omega})]_k dz, \quad i,j = 4,5 \tag{10}$$

where α_s is the shear correction factor and is assumed as 5/6. Now, the mass per unit area is denoted by P and is given by

$$P(\overline{\omega}) = \sum_{k=1}^{n} \int_{z_{k-1}}^{z_k} \rho(\overline{\omega}) dz \tag{11}$$

The element mass matrix is expressed as

$$[M_e(\overline{\omega})] = \int_{Vol} [N][P(\overline{\omega})][N] d(vol) \tag{12}$$

The element stiffness matrix is given by

$$[K_e(\overline{\omega})] = \int_{-1}^{1} \int_{-1}^{1} [B(\overline{\omega})]^T [D(\overline{\omega})][B(\overline{\omega})] d\xi \, d\eta \tag{13}$$

The Hamilton's principle [39] is employed to study the dynamic nature of the composite structure. The principle used for the Lagrangian which is defined as

$L_f = T - U - W$ where T, U and W are total kinetic energy, total strain energy and total potential of the applied load, respectively. The Hamilton's principle applicable to non-conservative system can be expressed as,

$$\delta H = \int_{t_i}^{t_f} [\delta T - \delta U - \delta W] dt = 0 \tag{14}$$

The energy functional for Hamilton's principle is the Lagrangian (L_f) which includes kinetic energy (T) in addition to potential strain energy (U) of an elastic body. The expression for kinetic energy of an element is given by

$$T = \frac{1}{2} \{\dot{\delta}_e\}^T [M_e(\overline{\omega})] + [C_e(\overline{\omega})]\{\delta_e\} \tag{15}$$

The potential strain energy for an element of a plate can be expressed as,

$$U = U_1 + U_2 = \frac{1}{2} \{\delta_e\}^T [K_e(\overline{\omega})]\{\delta_e\} \tag{16}$$

The Langrange's equation of motion is given by

$$\frac{d}{dt}\left[\frac{\partial L_f}{\partial \delta_e}\right] - \left[\frac{\partial L_f}{\partial \delta_e}\right] = \{F_e\} \tag{17}$$

where $\{F_e\}$ is the applied external element force vector of an element and L_f is the Lagrangian function. Substituting $L_f = T - U$, and the corresponding expressions for T and U in Lagrange's equation, one obtains the dynamic equilibrium equation for free vibration of each element in the following form [40]

$$[M_e(\overline{\omega})]\{\ddot{\delta}_e\} + [K_e(\overline{\omega})]\{\delta_e\} = 0 \tag{18}$$

After assembling all the element matrices and the force vectors with respect to the common global coordinates, the resulting equilibrium equation is obtained. For the purpose of this study, the finite element model is developed for different element types and finite element discretization and nodal positions of the driving point and measurement point. Considering randomness of input parameters like ply-orientation angle, thickness, elastic modulus and mass density etc., the equation of motion of a linear free vibration system with n degrees of freedom can expressed as

$$[M(\overline{\omega})]\ddot{\delta}(t) + [K(\overline{\omega})]\delta(t) = 0 \tag{19}$$

where $K(\overline{\omega}) \in R^{n \times n}$ is the elastic stiffness matrix, $M(\overline{\omega}) \in R^{n \times n}$ is the mass matrix and $\delta(t) \in R^n$ is the vector of generalized coordinates. The governing equations are derived based on Mindlin's theory incorporating rotary inertia, transverse shear deformation [41] using an eight noded isoparametric plate bending element [42]. The composite cantilever plate is assumed to be under free vibration and the natural frequencies of the system are obtained as:

$$\omega_j^2(\overline{\omega}) = \frac{1}{\lambda_j(\overline{\omega})} \quad \text{where } j = 1, \ldots, n_r \tag{20}$$

Here $\lambda_j(\overline{\omega})$ is the jth eigenvalue of matrix $A = K^{-1}(\overline{\omega})M(\overline{\omega})$ and n_r indicates the number of modes retained in this analysis.

3. Polynomial neural network

In general, the polynomial neural network (PNN) algorithm [43–45] is the advanced succession of Group Method of Data Handling (GMDH) method wherein different linear, modified quadratic, cubic polynomials are used. By choosing the most significant input variables and polynomial order among various types of forms available, the best partial description (PD) can be obtained based on selection of nodes of each layer and generation of additional layers until the best performance is reached. Such methodology leads to an optimal PNN structure wherein the input–output data set can be expressed as

$$(X_i, Y_i) = (x_{1i}, x_{2i}, x_{3i}, \ldots x_{ni}, y_i) \quad \text{where } i = 1,2,3 \ldots n \tag{21}$$

By computing the polynomial regression equations for each pair of input variable x_i and x_j and output Y of the object system which desires to modeling

$$Y = A + Bx_i + Cx_j + Dx_i^2 + Ex_j^2 + Fx_i x_j \quad \text{where } i,j = 1,2,3 \ldots n \tag{22}$$

where A, B, C, D, E, F are the coefficients of the polynomial equation. This provides $n(n-1)/2$ high-order variables for predicting the output Y in place of the original n variables $(x_1, x_2, \ldots, x_n)$. After finding these regression equations from a set of input–output observations, we then find out which ones to save. This gives the best predicted collection of quadratic regression models. We now use each of the quadratic equations that we have just computed and generate

new independent observations that will replace the original observations of the variables $(x_1, x_2, \ldots, x_n)$. From these new independent variables we will combine them exactly as we did before. That is, we compute all of the quadratic regression equations of Y versus these new variables. This will provide a new collection of $n(n-1)/2$ regression equation for predicting Y from the new variables, which in turn are estimates of Y from above equations. Now the best of new estimates is selected to generate new independent variables from selected equations to replace the old, and combine all pair of these new variables. This process is continued until the regression equations begin to have a poorer predictability power than did the previous ones. In other words, it is the time when the model starts to become overfitted. The estimated output $\hat{Y}_i$ can be further expressed as

$$\hat{Y} = \hat{f}(x_1, x_2, x_3, \ldots x_n) = A_0 + \sum_{i=1}^{n} B_i x_i + \sum_{i=1}^{n}\sum_{j=1}^{n} C_{ij} x_i x_j + \sum_{i=1}^{n}\sum_{j=1}^{n}\sum_{k=1}^{n} D_{ijk} x_i x_j x_k + \cdots \quad \text{where } i, j, k = 1, 2, 3 \ldots n \tag{23}$$

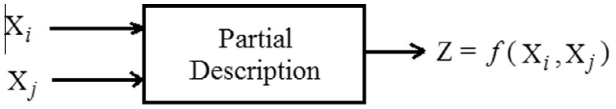

Fig. 2. Taxonomy for architectures of PNN.

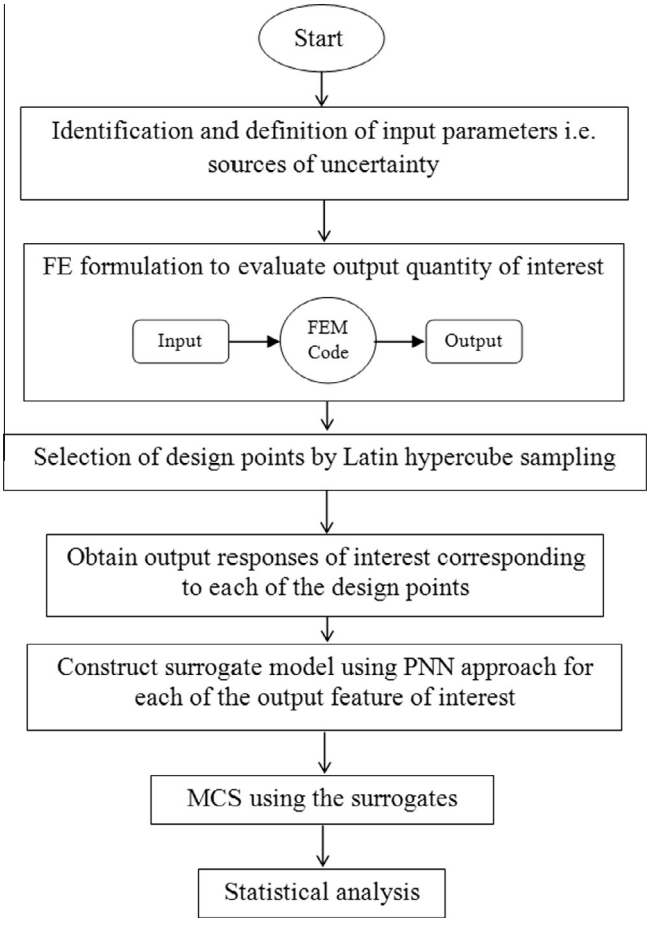

Fig. 3. Flowchart of stochastic natural frequency analysis using PNN model.

where $X(x_1, x_2, \ldots, x_n)$ is the input variables vector and $P(A_0, B_i, C_{ij}, D_{ijk}, \ldots)$ is vector of coefficients or weight of the Ivakhnenko polynomials. Components of the input vector X can be independent variables, functional forms or finite difference terms. This algorithm allows to find simultaneously the structure of model and model system output on the values of most significant inputs of the system. The following steps are to be performed for the framework of the design procedure of PNN:

Step 1: *Determination of input variables:* Define the input variables as $x_i = 1, 2, 3, \ldots n$ related to output variable Y. If required, the normalization of input data is also completed.

Step 2: *Create training and testing data*: Create the input–output data set (n) and divide into two parts, namely, training data (n_{train}) and testing data (n_{test}) where $n = n_{train} + n_{test}$. The training data set is employed to construct the PNN model including an estimation of the coefficients of the partial description of nodes situated in each layer of the PNN. Next, the testing data set is used to evaluate the estimated PNN model.

Step 3: *Selection of structure*: The structure of PNN is selected based on the number of input variables and the order of *PD* in each layer. Two kinds of PNN structures, namely a basic PNN and a modified PNN structure are distinguished. The basic taxonomy for the architectures of PNN structure is furnished in Fig. 2.

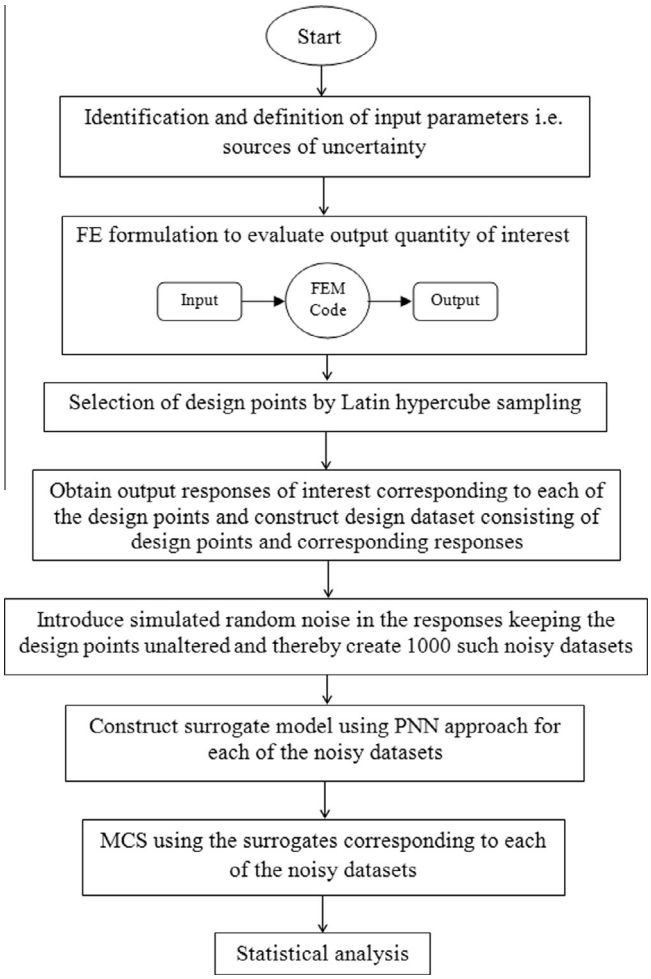

Fig. 4. Flowchart for analyzing the effect of noise on uncertainty quantification algorithm based on PNN.

Step 4: *Determination of number of input variables and order of the polynomial*: Determine the regression polynomial structure of a *PD* related to PNN structure. The input variables of a node from n input variables $x_1, x_2, x_3, \ldots x_n$ are selected. The total number of *PD*s located at the current layer differs according to the number of the selected input variables from the nodes of the preceding layer. This results in $k = n!/(n! - r!)r!$ nodes, where r is the number of the chosen input variables. The choice of the input variables and the order of a *PD* itself help to select the best model with respect to the characteristics of the data, model design strategy, nonlinearity and predictive capability.

Step 5: *Estimation of coefficients of PD*: The vector of coefficients A_i is derived by minimizing the mean squared error between Y_i and $\hat{Y}_i$.

$$PI = \frac{1}{n_{train}} \sum_{i=1}^{n_{train}} (Y_i - \hat{Y}_i)^2 \tag{24}$$

where PI represents a criterion which uses the mean squared differences between the output data of original system and the output data of the model. Using the training data subset, this gives rise to the set of linear equations

$$Y = \sum_{i=1}^{n} X_i A_i \tag{25}$$

The coefficients of the *PD* of the processing nodes in each layer are derived in the form

$$A_i = [X_i^T X_i]^{-1} X_i^T Y \tag{26}$$

where, $Y = [y_1, y_1, y_1, y_1, \ldots, y_{n_{train}}]^T$

$X_i = [x_{1i}, x_{2i}, x_{3i} \ldots X_{ki} \ldots X_{train\,i}]^T$

$X_{ki}^T = [x_{ki1} x_{ki2} \ldots x_{kin} \ldots x_{ki1}^m x_{ki2}^m \ldots x_{kin}^m]^T$

$A_i = [A_{0i}\, A_{1i}\, A_{2i} \ldots A_{n'i}]^T$

with the following notations i as the node number, k as the data number, n_{train} as the number of the training data subset, n as the number of the selected input variables, m as the maximum order, and n' as the number of estimated coefficients. This procedure is implemented repeatedly for all nodes of the layer and also for all layers of PNN starting from the input layer and moving to the output layer.

Step 6: *Selection of PDs with the best predictive capability*: Each *PD* is estimated and evaluated using both the training and testing data sets. Then we compare these values and choose several PDs, which give the best predictive performance for the output variable. Usually a predetermined number W of PDs is utilized.

Step 7: *Check the stopping criterion*: The stopping condition indicates that a sufficiently good PNN model is accomplished at the previous layer, and the modeling can be terminated. This condition reads as $PI_j > PI^*$ where PI_j is a minimal identification error of the current layer whereas PI^* denotes a minimal identification error that occurred at the previous layer.

Step 8: *Determination of new input variables for the next layer*: If PI_j (the minimum value in the current layer) has not been satisfied (so the stopping criterion is not satisfied), the model has to be expanded. The outputs of the preserved *PD*s serve as new inputs to the next layer.

Table 1
Convergence study for non-dimensional fundamental natural frequencies [$\omega = \omega_n L^2 \sqrt{(\rho/E_1 t^2)}$] of three layered (θ°/−θ°/θ°) graphite–epoxy composite plates, $a/b = 1$, $b/t = 100$, considering $E_1 = 138$ GPa, $E_2 = 8.96$ GPa, $G_{12} = 7.1$ GPa, $\mu = 0.3$.

Ply angle, θ	Present FEM (4 × 4)	Present FEM (6 × 6)	Present FEM (8 × 8)	Present FEM (10 × 10)	Qatu and Leissa [52]
0°	1.0112	1.0133	1.0107	1.004	1.0175
45°	0.4591	0.4603	0.4603	0.4604	0.4613
90°	0.2553	0.2567	0.2547	0.2542	0.2590

Table 2
Convergence study of first three natural frequencies (rad/s) due to individual and combined variation of ply-orientation angle, thickness, elastic modulus and mass density for angle-ply (45°/−45°/45°) composite cantilever plate.

Input variation	Values	f_1				f_2				f_3			
		MCS (10,000)	PNN (sample run)			MCS (10,000)	PNN (sample run)			MCS (10,000)	PNN (sample run)		
			256	512	1024		256	512	1024		256	512	1024
$\theta(\overline{\omega})$	Max	23.7997	23.5643	23.6540	24.0071	65.6675	65.5571	65.5471	65.6788	146.5351	145.0771	144.8005	145.7029
	Min	19.3219	19.4239	19.3018	19.3018	61.5809	61.8885	61.6920	61.6920	120.0259	121.4107	120.5559	120.5559
	Mean	21.4006	21.3656	21.4225	21.4033	63.7467	63.7190	63.7624	63.7468	133.2984	133.1224	133.4215	133.3062
	SD	0.9154	0.9342	0.9553	0.9412	0.8435	0.8522	0.8750	0.8567	5.3979	5.5109	5.6018	5.4922
$t_s(\overline{\omega})$	Max	23.5059	23.4940	23.5030	23.5057	70.2353	70.2008	70.2268	70.2347	146.4340	146.3612	146.4165	146.4328
	Min	19.2412	19.2529	19.2416	19.2445	57.6165	57.6511	57.6179	57.6263	120.1910	120.2629	120.1938	120.2113
	Mean	21.3736	21.3740	21.3762	21.3710	63.9269	63.9280	63.9347	63.9192	133.3144	133.3168	133.3306	133.2983
	SD	1.2313	1.2332	1.2325	1.2334	3.6434	3.6489	3.6468	3.6495	7.5772	7.5887	7.5843	7.5899
$E_1(\overline{\omega})$	Max	21.7663	21.8053	21.7723	21.8053	65.5082	65.6505	65.5334	65.6505	135.3713	135.5586	135.3602	135.5586
	Min	20.9694	20.9761	20.9342	20.9252	62.2682	62.3001	62.1369	62.1085	131.1839	131.2722	131.0464	130.9809
	Mean	21.3660	21.3623	21.3725	21.3666	63.8962	63.8856	63.9198	63.9002	133.2701	133.2431	133.3110	133.2704
	SD	0.1503	0.1617	0.1637	0.1645	0.5986	0.6491	0.6535	0.6501	0.8332	0.8689	0.8878	0.8793
$\rho(\overline{\omega})$	Max	22.3574	22.3099	22.4109	22.4276	66.8698	66.7277	67.0298	67.0797	139.4515	139.1552	139.7852	139.8893
	Min	20.5627	20.4647	20.5257	20.4647	61.5019	61.2089	61.3913	61.2089	128.2573	127.6462	128.0266	127.6462
	Mean	21.3835	21.3857	21.3691	21.3820	63.9570	63.9636	63.9138	63.9524	133.3771	133.3908	133.2871	133.3675
	SD	0.3609	0.3614	0.3601	0.3579	0.9897	1.0810	1.0770	1.0707	2.0639	2.2543	2.2461	2.2328
$\theta, t_s, E_1, \rho(\overline{\omega})$	Max	26.3531	25.8323	26.0243	26.0914	74.7603	72.5097	73.4380	74.2836	162.0763	158.5399	161.3411	161.3409
	Min	16.9109	18.0873	17.3134	17.3031	53.9388	54.7321	54.9025	54.9022	106.2299	112.3293	108.4457	108.4450
	Mean	21.3907	21.4701	21.4453	21.4557	63.7304	63.9235	63.9352	63.9335	133.2458	133.7428	133.6132	133.6546
	SD	1.6029	1.6241	1.5990	1.5759	3.9481	4.0223	4.0245	3.9509	9.6781	9.8289	9.6679	9.5026

4. Stochastic approach using PNN model

Layer-wise stochasticity in material and geometric properties are considered as input parameters for stochastic natural frequency analysis of composite plates. The individual and combined cases of layer-wise random variations considered in the present analysis are as follows:

(a) Variation of ply-orientation angle only: $\theta(\overline{\omega}) = \{\theta_1\theta_2\theta_3 \dots \theta_i \dots \theta_l\}$
(b) Variation of thickness only: $t(\overline{\omega}) = \{t_1t_2t_3 \dots t_i \dots t_l\}$
(c) Variation of elastic modulus only: $E_1(\overline{\omega}) = \{E_{1(1)}E_{1(2)}E_{1(3)} \dots E_{1(i)} \dots E_{1(l)}\}$
(d) Variation of mass density only: $\rho(\overline{\omega}) = \{\rho_1\rho_2\rho_3 \dots \rho_i \dots \rho_l\}$
(e) Combined variation of ply orientation angle, thickness, elastic modulus (longitudinal)and mass density:

$$g\{\theta(\overline{\omega}), t(\overline{\omega}), E_1(\overline{\omega}), \rho(\overline{\omega})\} = \{\Phi_1(\theta_1 \dots \theta_l), \Phi_2(t_1 \dots t_l), \Phi_3(E_{1(1)} \dots E_{1(l)}), \Phi_4(\rho_1 \dots \rho_l)\}$$

where θ_i, t_i, $E_{1(i)}$ and ρ_i are the ply orientation angle, thickness, elastic modulus along longitudinal direction and mass density, respectively and 'l' denotes the number of layer in the laminate. In the present study it is assumed that the distribution for randomness of input parameters exists within a certain band of tolerance with their deterministic values. $\pm5^\circ$ for ply orientation angle and $\pm10\%$ tolerance for material properties and thickness from deterministic values are considered. The flowchart of the proposed stochastic natural frequency analysis using PNN model is shown in Fig. 3. Latin hypercube sampling [43] is employed for generating sample points to ensure the representation of all portions of the vector space. In Latin hypercube sampling, the interval of each dimension is divided into m non-overlapping intervals having equal probability considering a uniform distribution, so the intervals should have equal size. Moreover, the sample is chosen randomly from a uniform distribution with a point in each interval, in each dimension and the random pair is selected considering equal likely combinations for the point from each dimension. Subsequently to portray the effect of noise on the proposed PNN based uncertainty quantification algorithm, different levels of noise is introduced as described in Fig. 4.

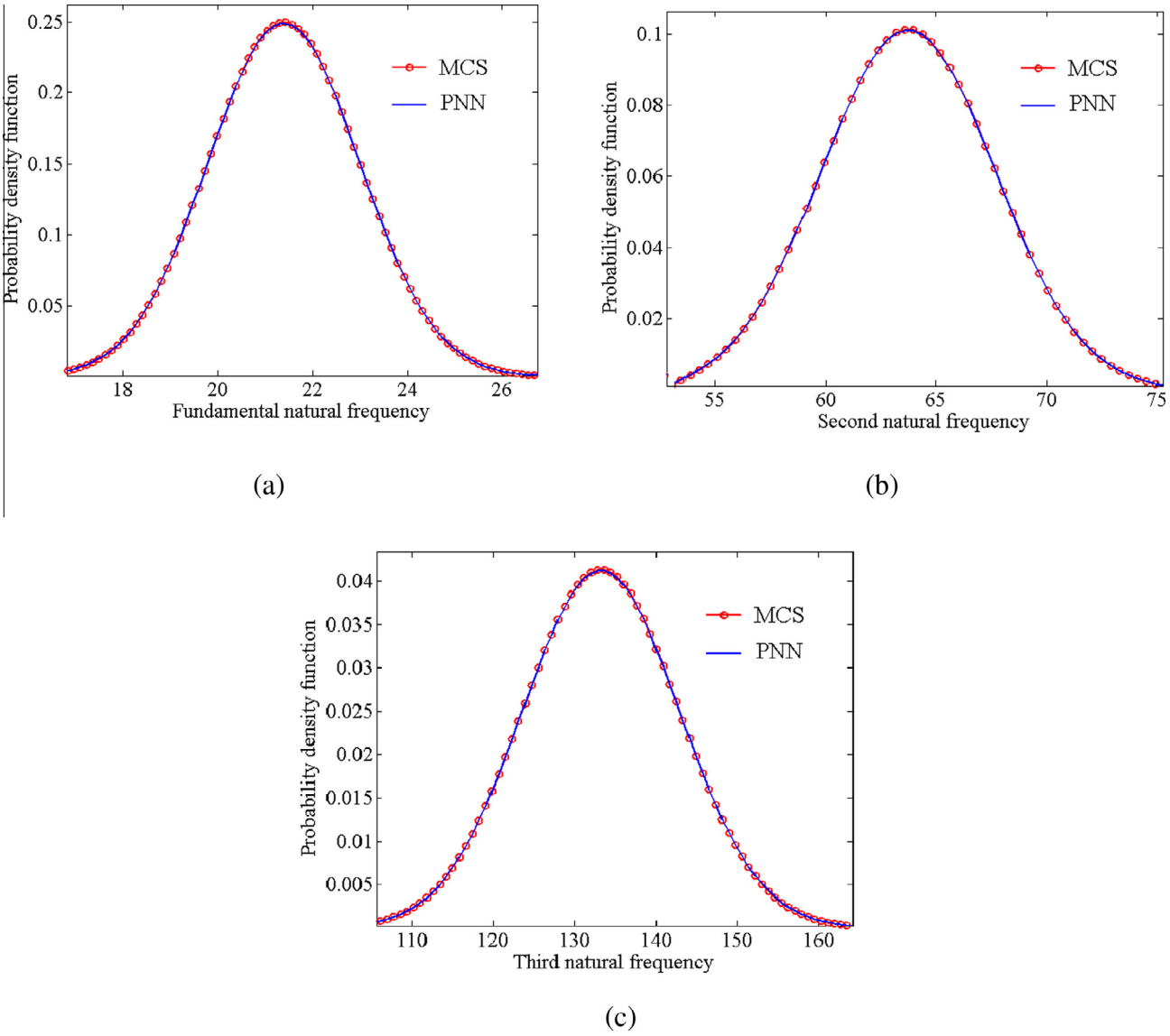

Fig. 5. Probability density function of first three stochastic natural frequencies (rad/s) using PNN approach for combined variation of ply angle, ply-thickness, longitudinal elastic modulus and mass density of angle-ply ($45^\circ/-45^\circ/45^\circ$) composite cantilever plate.

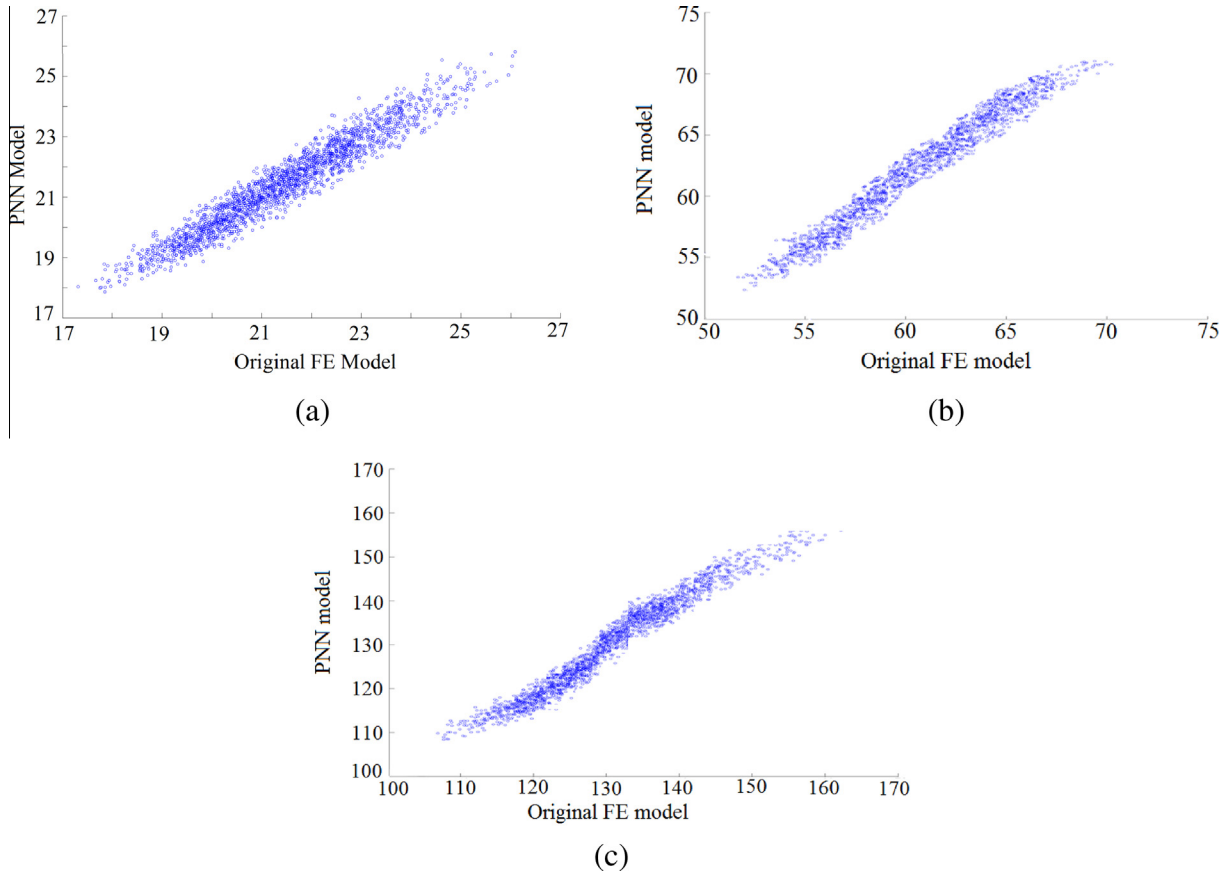

Fig. 6. Scatter plot for first three natural frequencies (rad/s) with respect to PNN model and original finite element model for combined variation of ply angle, ply-thickness, longitudinal elastic modulus and mass density of angle-ply (45°/−45°/45°) composite cantilever plate.

In the proposed approach, a Gaussian white noise with a specific multiplication factor (Var) is introduced in the set of output responses, which is used for PNN model formation

$$f_{ijN} = f_{ij} + \mathrm{Var} \times \xi_{ij} \tag{28}$$

where f denotes natural frequency with the subscript i and j as frequency number and sample number, respectively.ξ_{ij} is a function that generates normally distributed random numbers. Subscript 'N' is used here to indicate the noisy frequency. Physical quantities that are expected to be the sum of many independent processes often have distributions that are nearly normal [46]. Therefore, Gaussian distribution has been adopted in this study to explore the effect of random noise. Thus, simulated noisy dataset (i.e. the sampling matrix for PNN model formation) is formed by introducing pseudo random noise in the responses, while the input design points are kept unaltered. Subsequently for each dataset, PNN based MCS is carried out to quantify the uncertainty of composite plates as described in Fig. 4. Effects of noise are found to be accounted in several other studies in available literature [47–49] dealing with deterministic analysis. Recently noise is found to be accounted in uncertainty propagation using Kriging [50]. Assessment of PNN based uncertainty propagation algorithm under the effect of noise is the first attempt of its kind to the best of the authors' knowledge. The effect of such simulated noise can be regarded as considering other sources of uncertainty (except the commonly considered stochasticity in material and geometric parameters) such as error in measurement of responses, error in modeling and computer simulation and various other epistemic uncertainties involved with the system. It is difficult to quantitatively account the above mentioned sources of uncertainty and therefore, often ignored in most of the available literature. Thus, the kind of analysis carried out here will provide a comprehensive idea about the robustness of PNN based uncertainty quantification algorithm under noisy data.

5. Results and discussion

In this study, three layered graphite–epoxy symmetric angle-ply laminated composite cantilever plates are considered. The length, width and thickness of the composite laminate considered in the present analysis are 1 m, 1 m and 5 mm, respectively.

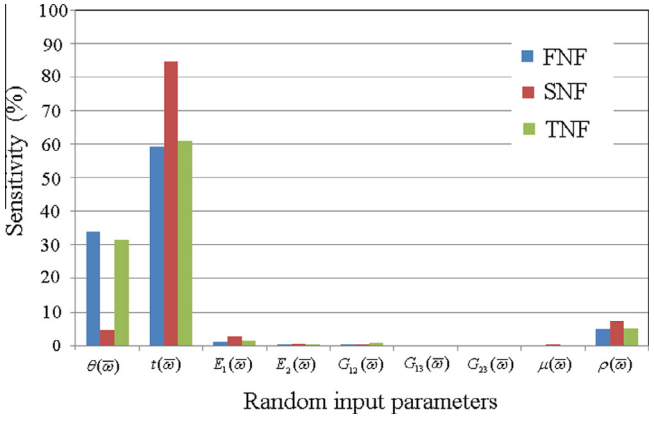

Fig. 7. Sensitivity of input parameters corresponding to fundamental (FNF), second (SNF) and third (TNF) natural frequencies for angle-ply (45°/−45°/45°) composite cantilever plate.

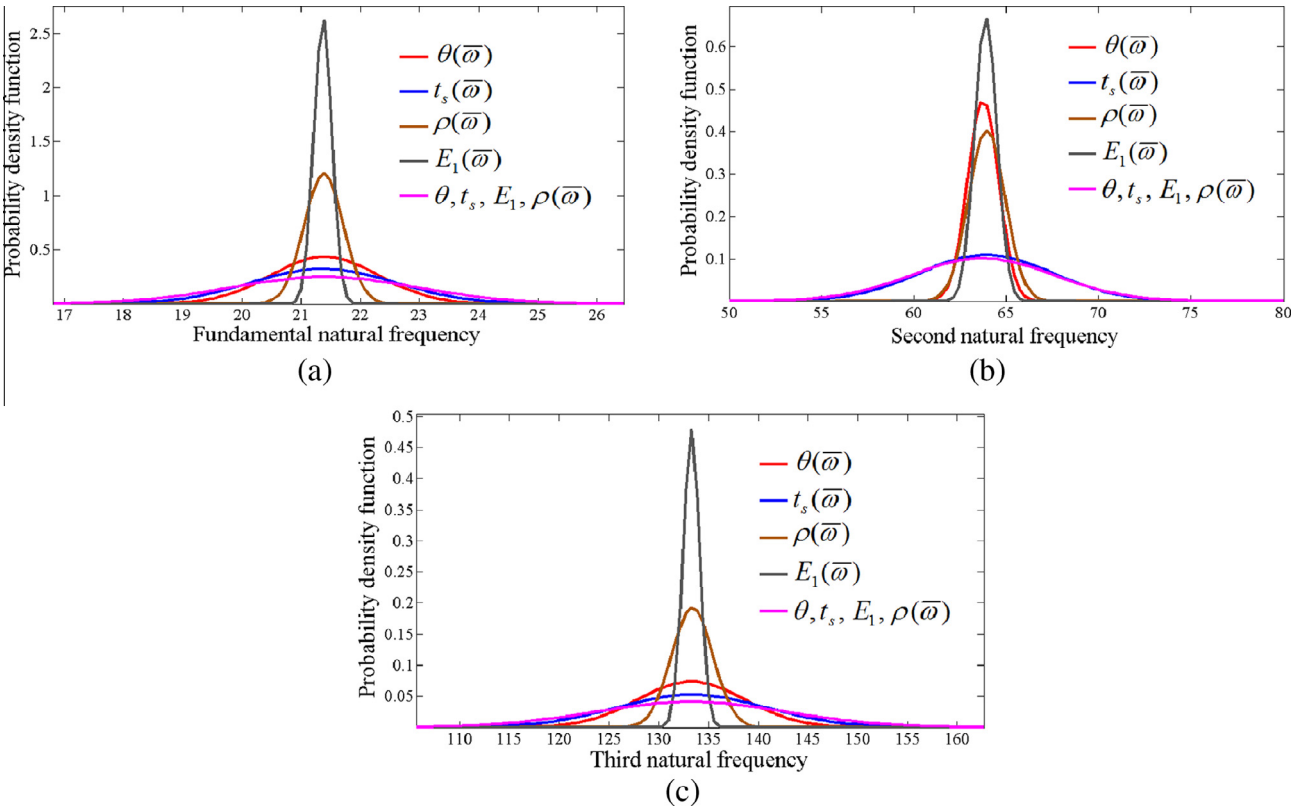

Fig. 8. Probability density function for first three natural frequencies (rad/s) due to individual and combined variation of ply-orientation angle, thickness, elastic modulus and mass density for angle-ply (45°/−45°/45°) composite cantilever plate.

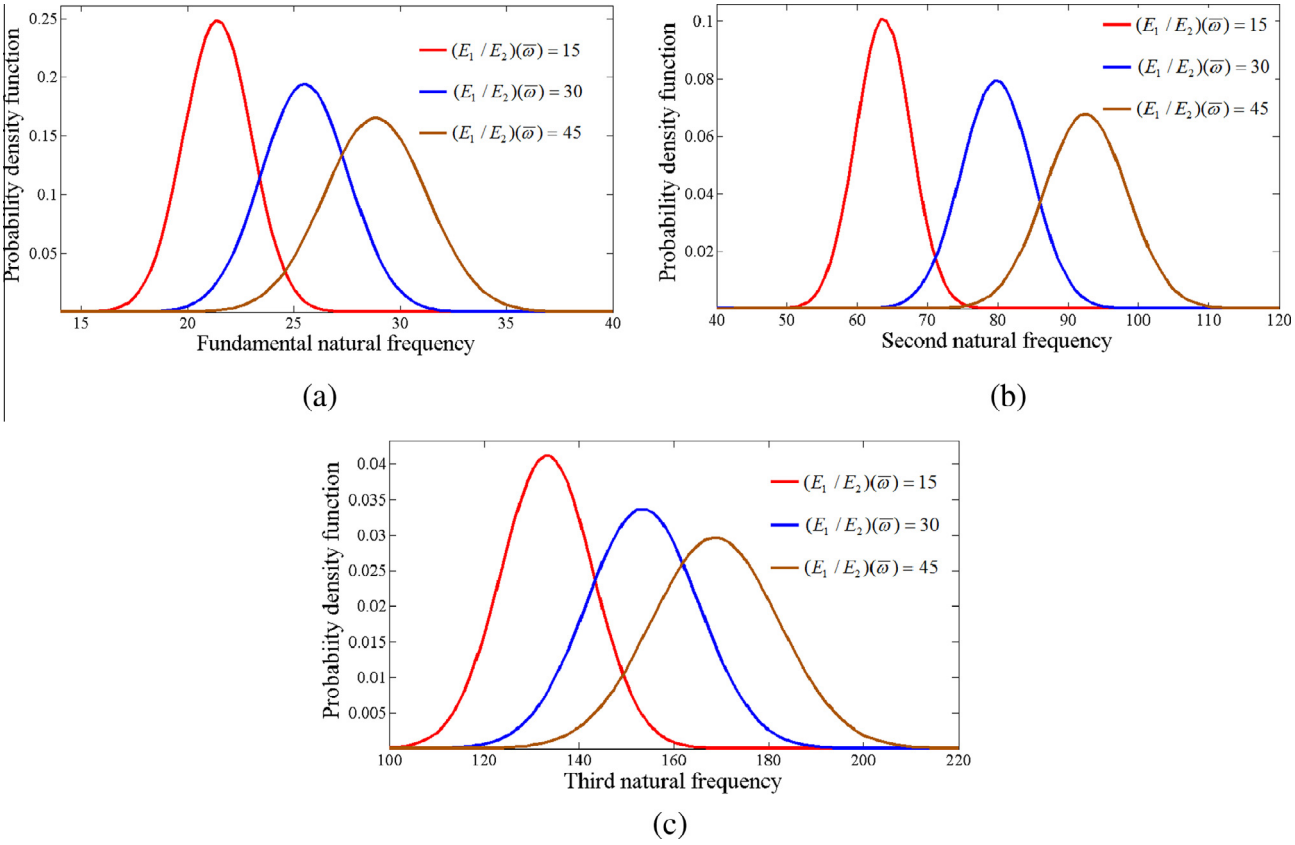

Fig. 9. Effect of degree of orthogonality on stochastic (a) fundamental (b) second and (c) third natural frequencies (rad/s) with respect to PNN model for combined variation of angle-ply (45°/−45°/45°) composite cantilever plate.

Material properties of graphite–epoxy composite [51] considered with deterministic mean value as $E_1 = 138.0$ GPa, $E_2 = 8.96$ GPa, $G_{12} = 7.1$ GPa, $G_{13} = 7.1$ GPa, $G_{23} = 2.84$ GPa, $\mu = 0.3$, $\rho = 1600$ kg/m^3. A discretization of (6×6) mesh on plan area with 36 elements 133 nodes with natural coordinates of an isoparametric quadratic plate bending element are considered for the present FEM approach. The finite element mesh size is finalized using a convergence study as shown in Table 1. For full scale MCS, the number of original finite element analysis is same as the sampling size. In general for complex composite structures, the performance function is not available as an explicit function of the random variables. The random response in terms of natural frequencies of the composite structure can only be evaluated numerically at the end of a structural analysis procedure such as the finite element method which is often time-consuming and computationally expensive. The present PNN method is employed to develop a predictive and representative surrogate model relating each natural frequency to a number of input variables. Thus the PNN model represents the result of structural analysis encompassing every possible combination of all stochastic input variables. From this mathematical model, thousands of combinations of all design variables can be created and performed using a pseudo analysis for each variable set, by adopting the corresponding predictive values.

A convergence study of sample size for PNN model formation with respect to direct MCS is shown in Table 2 for the first three stochastic natural frequencies due to individual and combined variation of ply-orientation angle, thickness, elastic modulus and mass density. It is a common practice to choose the sample size as 2^N, where N is a positive integer. In the present article we have shown typical results of convergence study for $N = 8$, 9 and 10 due to paucity of space. By analyzing the statistical parameters presented in the Table 2 it is evident that sample size of 256 and 512 are adequate to form PNN model for individual and combined variation cases respectively.

The probability density function (PDF) is plotted as the benchmark of bottom line results in this article. To illustrate the validation of results of the proposed PNN based approach with respect to direct MCS, natural frequencies corresponding to first three modes are considered. The probability density function plots comparing MCS with PNN and the scatter plots verifying the present PNN model corresponding to the first three modes are presented in

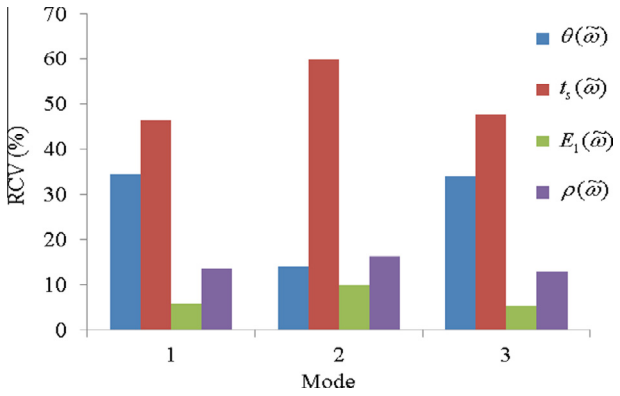

Fig. 11. Relative coefficient of variation (RCV) with respect to first three natural frequencies for angle-ply (45°/−45°/45°) composite cantilever plate.

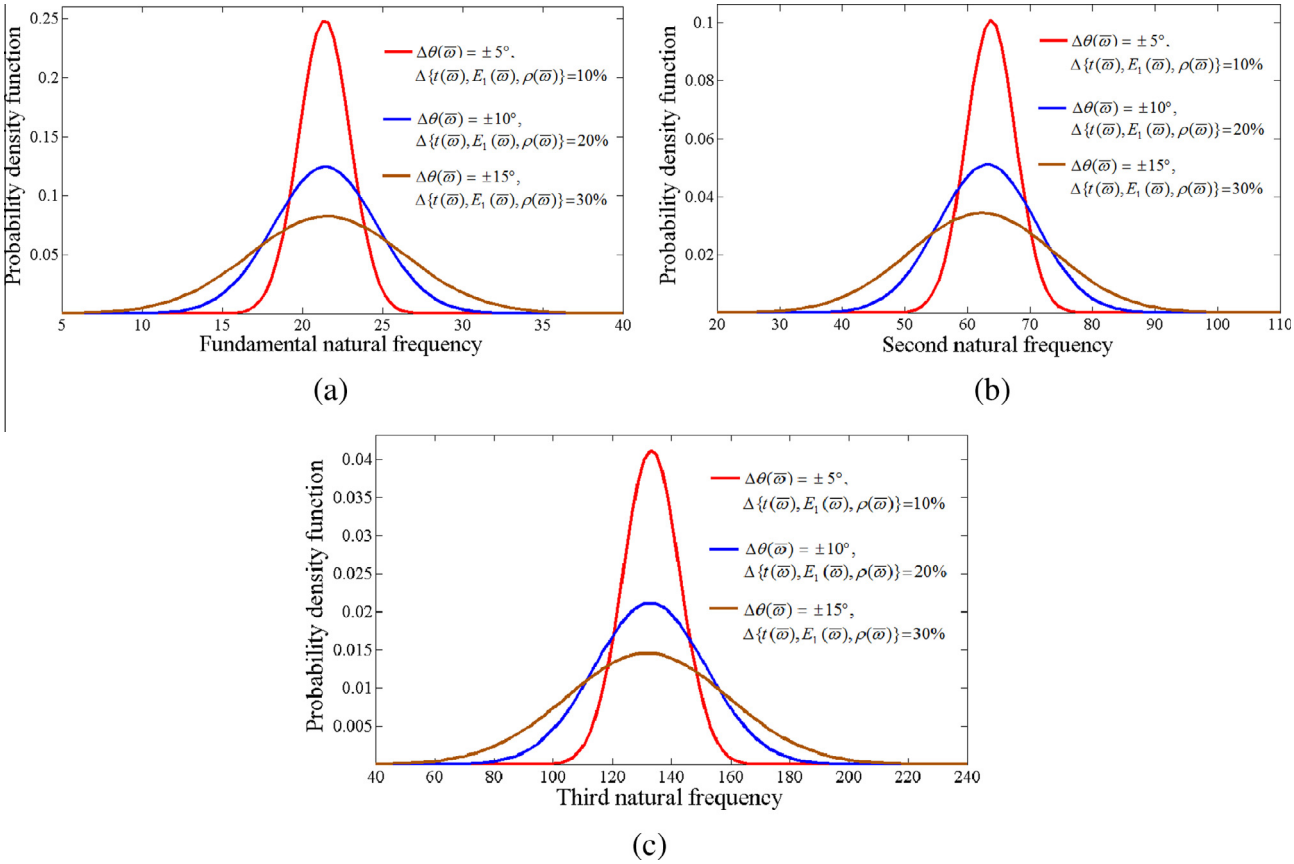

Fig. 10. Effect of variation of input parameters on stochastic (a) fundamental (b) second and (c) third natural frequencies (rad/s) with respect to PNN model for combined variation of angle-ply (45°/−45°/45°) composite cantilever plate.

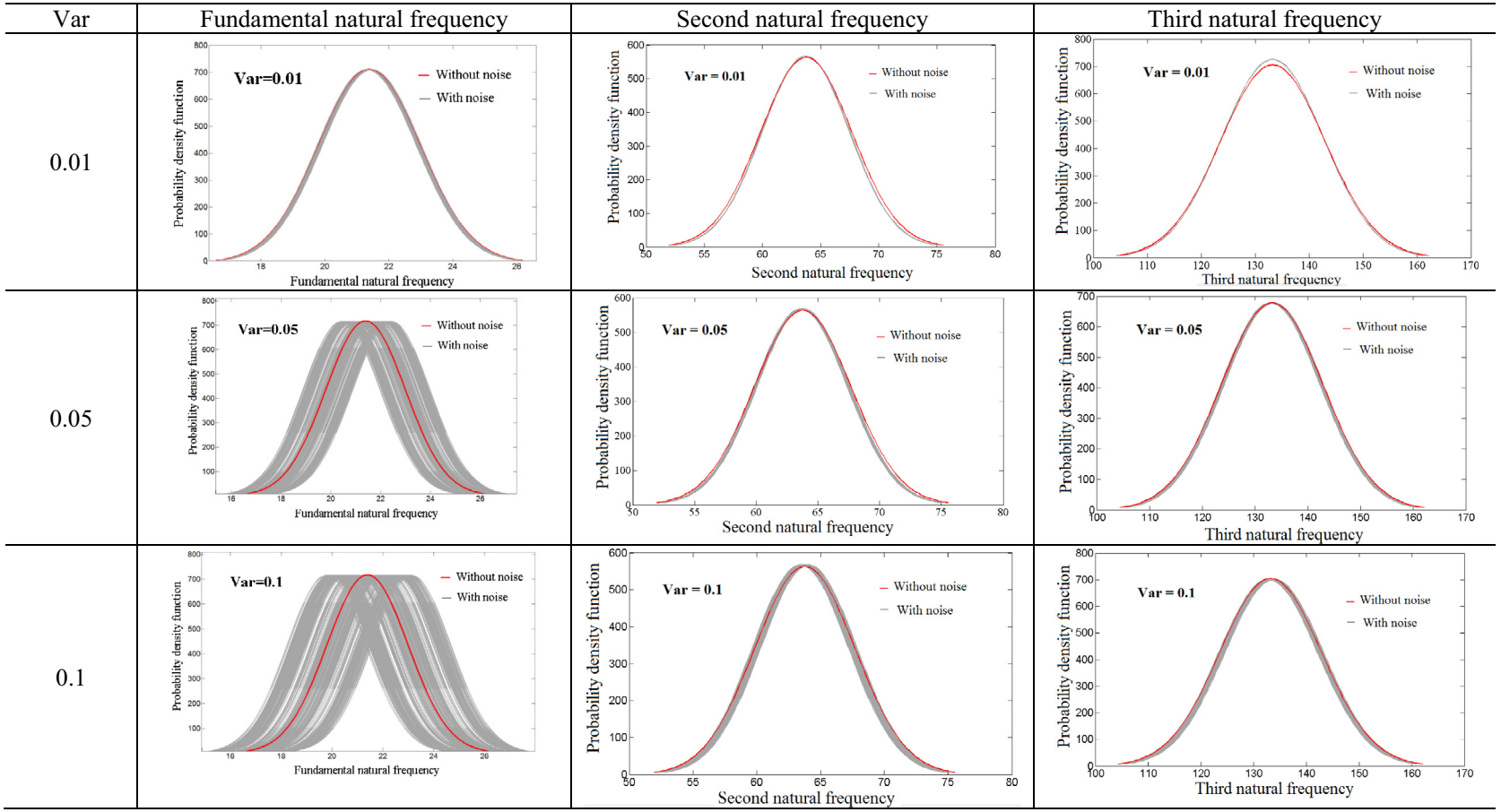

Fig. 12. Effect of noise on PNN based uncertainty quantification for first three natural frequencies (rad/s) of laminated composite plates due to combined variation of ply-orientation angle, thickness, elastic modulus and mass density for angle-ply composite cantilever plate.

Var	Fundamental natural frequency	Second natural frequency	Third natural frequency
0.2	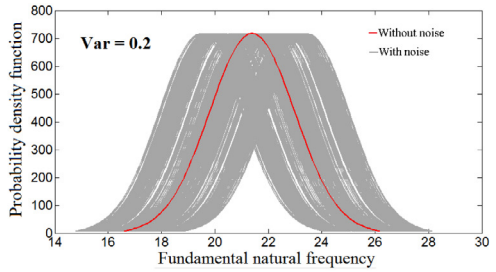	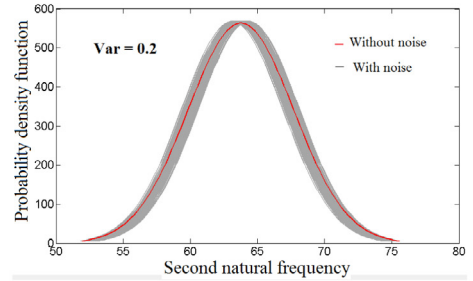	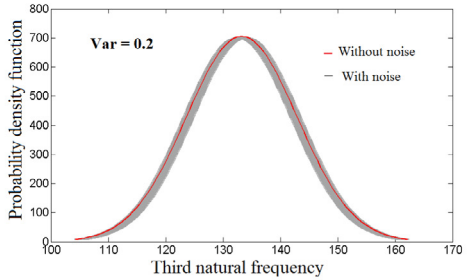
0.5	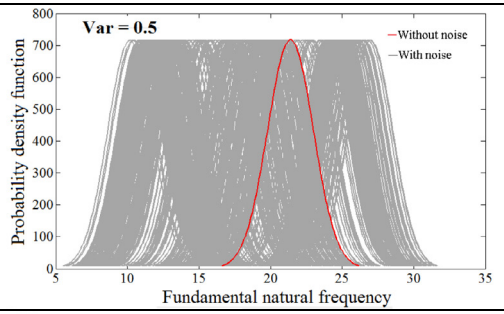	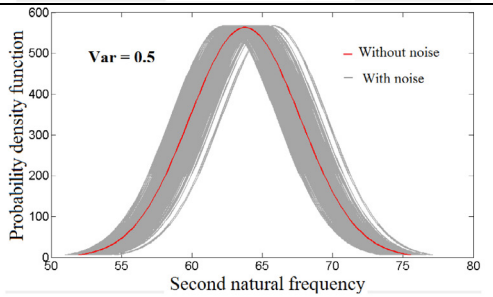	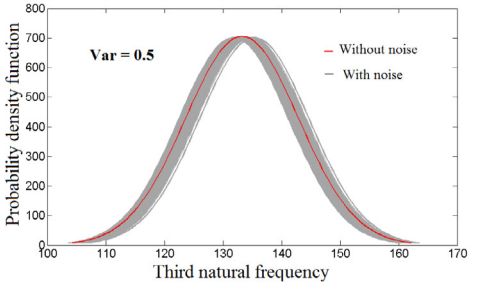
1.0	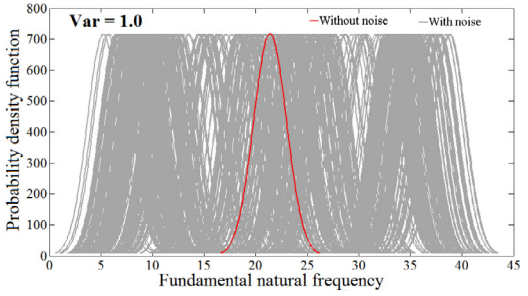	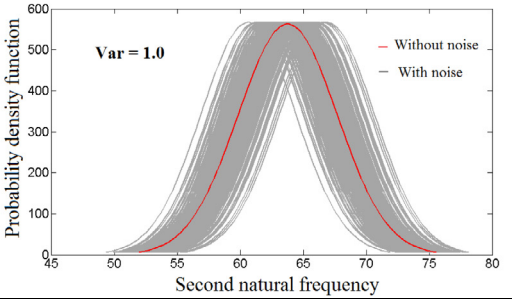	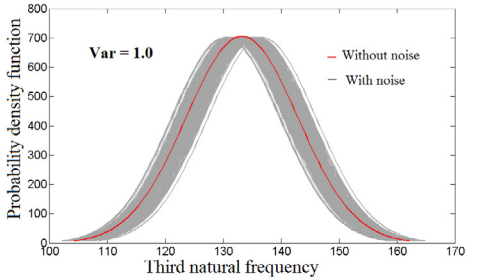

Fig. 12 (*continued*)

Figs. 5 and 6 respectively. It is evident that the results of the proposed PNN based approach are in good agreement with that of direct MCS simulations corroborating accuracy of the proposed approach. Several new results for stochastic analysis of composite plates are generated using the PNN based approach as presented in the subsequent paragraphs.

As presented in Fig. 7, the four most sensitive input parameters are identified as ply orientation angle, longitudinal elastic modulus, thickness and mass density using variance based global sensitivity analysis [47] while, the variation of other input parameters such as transverse elastic modulus, shear moduli and Poisson's ratio are found to have very little or negligible contribution on stochasticity of first three natural frequencies. For this reason the above mentioned four most sensitive input parameters are considered for analyzing combined stochasticity in the present analysis. The probability density function with respect to first three stochastic natural frequencies are plotted in Fig. 8 due to individual and combined variation of ply-orientation angle, thickness, elastic modulus and mass density for angle-ply composite cantilever plate. The combined variation of input parameters is observed to have the maximum influence on stochasticity of natural frequencies compared to individual variation of input parameters irrespective of modes. Moreover, this collective plots give a clear idea about the volatility in natural frequencies due to stochasticity in different individual parameters that in turn provides a sense of their relative influences on the responses of interest. The effect of degree of orthogonality on stochastic first three natural frequencies corresponding to combined variation of angle-ply ($45^\circ/-45^\circ/45^\circ$) composite cantilever plate is shown in Fig. 9. It is observed that as the ratio of longitudinal elastic modulus to transverse elastic modulus increases the fluctuation of stochastic natural frequencies also proportionately increases irrespective of modes. To ascertain the degree of proportional variation, a comparative study is carried out to map the variation of stochastic natural frequencies due to variation in input parameters in case of combined variation case. Three cases are considered namely, (a) $\pm5^\circ$ for ply orientation angle with subsequent $\pm10\%$ tolerance for material properties (b) $\pm10^\circ$ for ply orientation angle with subsequent $\pm20\%$ tolerance for material properties and (c) $\pm15^\circ$ for ply orientation angle with subsequent $\pm20\%$ tolerance for material properties from respective deterministic mean values as depicted in Fig. 10. It is evident that as the fluctuation of input parameters increases the sparsity of the stochastic output natural frequencies also increases while no notable variation of stochastic mean value of respective natural frequencies is identified due to the same.

To map the contribution of individual input parameters due to their individual variation, the relative coefficient of variation (RCV) for first three modes of frequencies are evaluated as shown in Fig. 11. The thickness of each layer of the laminate is identified as the relatively most effective input parameter, followed by ply orientation angle, mass density and elastic modulus E_1. It can be noted here that the results of RCV are in good agreement with Fig. 7. The effect of noise on PNN based uncertainty quantification algorithm (refer to Fig. 4) for the case of combined variation of all stochastic input parameters is furnished in Fig. 12. As the multiplication factor Var increases, the range of variations in the probability density function is also found to be increased. The fundamental natural frequency is identified to be the maximum noise-sensitive followed by the subsequent second and third natural frequencies. This is because of the fact that the range of magnitude increases with the increase in mode number and as magnitude of a particular frequency becomes higher the influence of same noise level would be lesser on that frequency.

6. Conclusions

The novelty of the present study includes incorporation of polynomial neural network based uncertainty propagation algorithm in laminated composite plates. Stochastic natural frequencies are analyzed considering layer-wise variation of individual as well as combined cases for random input parameters. Subsequently, the effect of noise on the proposed approach of uncertainty quantification is addressed. In this study, the uncertainty quantification of natural frequencies with uniform random input variables (such as ply orientation, ply-thickness and material properties) is formulated implicitly using finite element method and thereby PNN approach is incorporated to achieve computational efficiency. The computational time and cost is reduced by using the present PNN approach compared to conventional Monte Carlo simulation method. From the analyses presented in this article it is found that, as the percentage of variation of input parameters increases, the sparsity of the stochastic output natural frequencies also increases while no notable variation of stochastic mean value of respective natural frequencies is identified. The thickness parameter is found to be the most sensitive input parameter while longitudinal elastic modulus is observed as the least sensitive parameter. Interestingly, the stochastic fundamental frequency is identified to be the maximum noise-sensitive compared to higher natural frequencies. The PNN based approach for uncertainty quantification presented in this article can be extended to deal with more complex systems in future.

Acknowledgement

SN and SS gratefully acknowledge the financial support from Lloyd's Register Foundation Centre during this work.

References

[1] Leissa AW. Vibration of plates. NASA SP-160; 1969.
[2] Huang CS, McGee OG, Leissa AW. Exact analytical solutions for free vibrations of thick sectorial plates with simply supported radial edges. Int J Solids Struct 1994;31(11):1609–31.
[3] Reddy JN. A refined nonlinear theory of plates with transverse shear deformation. Int J Solids Struct 1984;20(9–10):881–96.
[4] Liew KM, Ng TY, Wang BP. Vibration of annular sector plates from three-dimensional analysis. J Acoust Soc Am 2001;110(1):233–42.
[5] Tornabene F, Viola E, Fantuzzi N. General higher-order equivalent single layer theory for free vibrations of doubly curved laminated composite shells and panels. Compos Struct 2013;104:94–117.
[6] Tornabene F, Fantuzzi N, Bacciocchi M. The local GDQ method applied to general higher-order theories of doubly-curved laminated composite shells and panels: the free vibration analysis. Compos Struct 2014;116:637–60.
[7] Fantuzzi N, Bacciocchi M, Tornabene F, Viola E, Ferreira AJM. Radial basis functions based on differential quadrature method for the free vibration analysis of laminated composite arbitrarily shaped plates. Compos B Eng 2015;78:65–78.
[8] Huang L, Sheikh AH, Ng CT, Griffith MC. An efficient finite element model for buckling of grid stiffened laminated composite plates. Compos Struct 2015;122:41–50.
[9] Shaker A, Abdelrahman WG, Tawfik M, Sadek E. Stochastic finite element analysis of the free vibration of laminated composite plates. Comput Mech 2008;41(4):493–501.
[10] Ganesan R. Free-vibration of composite beam-columns with stochastic material and geometric properties subjected to random axial loads. J Reinf Plast Compos 2005;24(1):69–91.
[11] Lal A, Singh BN. Stochastic nonlinear free vibration of laminated composite plates resting on elastic foundation in thermal environments. Comput Mech 2009;44(1):15–29.
[12] Sephvand K, Marburg S, Hardtke HJ. Uncertainty quantification in stochastic systems using polynomial chaos expansion. Int J Appl Mech 2010;2(2):305.
[13] Naveenthraj B, Iyengar NGR, Yadav D. Response of composite plates with random material properties using FEM and MCS. Adv Compos Mater 1998;7:219–37.
[14] Salim S, Yadav D, Iyengar NGR. Analysis of composite plates with random material characteristics. Mech Res Commun 1993;20(5):405–14.
[15] Onkar AK, Yadav D. Non-linear response statistics of composite laminates with random material properties under random loading. Compos Struct 2003;60(4):375–83.

[16] Giunta G, Carrera E, Belouettar S. Free vibration analysis of composite plates via refined theories accounting for uncertainties. Shock Vib 2011;18:537–54.
[17] Dey S, Mukhopadhyay T, Sahu SK, Li G, Rabitz H, Adhikari S. Thermal uncertainty quantification in frequency responses of laminated composite plates. Compos B Eng 2015;80:186–97.
[18] Dey S, Mukhopadhyay T, Adhikari S. Stochastic free vibration analysis of angle-ply composite plates – A RS-HDMR approach. Compos Struct 2015;122:526–36.
[19] Bui TQ, Nguyen MN. A moving Kriging interpolation-based meshfree method for free vibration analysis of Kirchhoff plates. Comput Struct 2011;89(3–4):380–94.
[20] Dey S, Mukhopadhyay T, Adhikari S. Stochastic free vibration analyses of composite shallow doubly curved shells – a Kriging model approach. Compos B Eng 2015;70:99–112.
[21] Xing YF, Wang YS, Shi L, Guo H, Chen H. Sound quality recognition using optimal wavelet-packet transform and artificial neural network methods. Mech Syst Signal Process 2016;66–67:875–92.
[22] Piotrowski AP, Napiorkowski MJ, Napiorkowski JJ, Osuch M. Comparing various artificial neural network types for water temperature prediction in rivers. J Hydrol 2015;529(1):302–15.
[23] Singh VP, Chakraverty S, Sharma RK, Sharma GK. Modeling vibration frequencies of annular plates by regression based neural network. Appl Soft Comput 2009;9(1):439–47.
[24] Spiridonakos MD, Chatzi EN. Metamodeling of dynamic nonlinear structural systems through polynomial chaos NARX models. Comput Struct 2015;157:99–113.
[25] Dey S, Mukhopadhyay T, Khodaparast HH, Kerfriden P, Adhikari S. Rotational and ply-level uncertainty in response of composite shallow conical shells. Compos Struct 2015;131:594–605.
[26] Dey S, Mukhopadhyay T, Khodaparast HH, Adhikari S. Fuzzy uncertainty propagation in composites using Gram–Schmidt polynomial chaos expansion. Appl Math Model. http://dx.doi.org/10.1016/j.apm.2015.11.03.
[27] Zjavka L. Wind speed forecast correction models using polynomial neural networks. Renewable Energy 2015;83:998–1006.
[28] Gómez-Ramírez E, Najim K, Ikonen E. Forecasting time series with a new architecture for polynomial artificial neural network. Appl Soft Comput 2007;7(4):1209–16.
[29] Zhang Y, Yin Y, Guo D, Yu X, Xiao L. Cross-validation based weights and structure determination of Chebyshev-polynomial neural networks for pattern classification. Pattern Recogn 2014;47(10):3414–28.
[30] Xin Yu, Chen Qingfeng. Convergence of gradient method with penalty for ridge polynomial neural network. Neurocomputing 2012;97:405–9.
[31] Xin Yu, Tang Lixia, Chen Qingfeng, Chenhua Xu. Monotonicity and convergence of asynchronous update gradient method for ridge polynomial neural network. Neurocomputing 2014;129:437–44.
[32] Roh Seok-Beom, Ahn Tae-Chon, Pedrycz Witold. Fuzzy linear regression based on polynomial neural networks. Expert Syst Appl 2010;39(10):8909–28.
[33] Roh SB, Oh SK, Pedrycz W. Design of fuzzy radial basis function-based polynomial neural networks. Fuzzy Sets Syst 2011;185(1):15–37.
[34] Huang W, Oh SK, Pedrycz W. Design of hybrid radial basis function neural networks (HRBFNNs) realized with the aid of hybridization of fuzzy clustering method (FCM) and polynomial neural networks (PNNs). Neural Networks 2014;60:166–81.
[35] Oh SK, Kim WD, Park BJ, Pedrycz W. A design of granular-oriented self-organizing hybrid fuzzy polynomial neural networks. Neurocomputing 2013;119:292–307.
[36] Fazel Zarandi MH, Türksen IB, Sobhani J, Ramezanianpour AA. Fuzzy polynomial neural networks for approximation of the compressive strength of concrete. Appl Soft Comput 2008;8(1):488–98.
[37] Maric I. Optimization of self-organizing polynomial neural networks. Expert Syst Appl 2013;40(11):4528–38.
[38] Dorn M, Braga ALS, Llanos CH, Coelho LS. A GMDH polynomial neural network-based method to predict approximate three-dimensional structures of polypeptides. Expert Syst Appl 2012;39(15):12268–79.
[39] Meirovitch L. Dynamics and control of structures. NY: John Wiley & Sons; 1992.
[40] Dey S, Karmakar A. Natural frequencies of delaminated composite rotating conical shells – a finite element approach. Finite Elem Anal Des 2012;56:41–51.
[41] Dey S, Karmakar A. Free vibration analyses of multiple delaminated angle-ply composite conical shells – a finite element approach. Compos Struct 2012;94(7):2188–96.
[42] Bathe KJ. Finite element procedures in engineering analysis. New Delhi: PHI; 1990.
[43] Schetinin V. Polynomial neural networks learnt to classify EEG signals, NIMIA-SC2001 – 2001 NATO advanced study institute on neural networks for instrumentation, measurement, and related industrial applications: study cases Crema, Italy; 9–20 October 2001.
[44] Mellit A, Drif M, Malek A. EPNN-based prediction of meteorological data for renewable energy systems. Revue des Energies Renouvelables 2010;13(1):25–47.
[45] Oh SK, Pedrycz W, Park BJ. Polynomial neural networks architecture: analysis and design. Comput Electr Eng 2003;29(6):703–25.
[46] Lyon A. Why are normal distributions normal? Br J Philos Sci 2014;65(3):621–49.
[47] Mukhopadhyay T, Chowdhury R, Chakrabarti A. Structural damage identification: a RS-HDMR approach. Adv Struct Eng 2016. http://dx.doi.org/10.1177/1369433216630370.
[48] Dey S, Mukhopadhyay T, Spickenheuer A, Adhikari S, Heinrich G. Bottom up surrogate based approach for stochastic frequency response analysis of laminated composite plates. Compos Struct 2016;140:712–27.
[49] Mukhopadhyay T, Dey TK, Chowdhury R, Chakrabarti A. Structural damage identification using response surface based multi-objective optimization: a comparative study. Arab J Sci Eng 2015;40(4):1027–44.
[50] Mukhopadhyay T, Naskar S, Dey S, Adhikari S. On quantifying the effect of noise in surrogate based stochastic free vibration analysis of laminated composite shallow shells. Compos Struct 2016;140:798–805.
[51] Qatu MS, Leissa AW. Natural frequencies for cantilevered doubly curved laminated composite shallow shells. Compos Struct 1991;17:227–55.
[52] Qatu MS, Leissa AW. Vibration studies for laminated composite twisted cantilever plates. Int J Mech Sci 1991;33(11):927–40.